Bulletin of Engineering Geology and the Environment (2025) 84:374
https://doi.org/10.1007/s10064-025-04398-6

ORIGINAL PAPER

# Determining the geometry of tailings dams using magnetic prospecting in the La Carolina mining district (southern Spain)

Rosendo Mendoza[1] · Javier Rey[2] · José Vilchez[2] · Francisco J. Martínez-Moreno[3] · M. Carmen Hidalgo[2]

Received: 8 June 2024 / Accepted: 22 April 2025



## Abstract

In the former mining district of La Carolina (southern Spain), waste materials were accumulated until the beginning of the 1980s without first waterproofing the substrate. Additionally, these mining dumps were abandoned without any type of restoration, which are conditions that present a significant risk of contamination of the surrounding soils and waters. Prior to carrying out the necessary work for isolating these residues, it is essential to know the geometry, thickness and distribution of wastes accumulated on the base substrate. For that purpose, in recent years, different indirect study techniques have been used, among which electrical tomography stands out. In this work, a complementary technique, magnetometry, both in its magnetic and gradiometric modalities, is used as an additional method to analyse the geometry and structure of a tailings dam. The results obtained with this methodology are compared with the results provided by electrical techniques, as well as with direct data from mechanical surveys and aerial photographs prior to waste deposition. Four total field magnetic anomaly profiles were selected for forward modelling using Mag2dc software. A correlation between total field magnetic anomaly values and changes in the accumulated thickness of mining waste was established. In this example, the lowest magnetic values coincide with the smallest thicknesses of the tailings dam. This comparative study shows the usefulness of magnetic prospecting in characterizing the base geometry of these mining structures and therefore the application to environmental characterization studies.


**Keywords** Sulfide ores · Tailings dams · Environmental hazard · Magnetometry · Magnetic susceptibility · La Carolina mining district

✉ Javier Rey
jrey@ujaen.es

Rosendo Mendoza
rmendoza@ujaen.es

José Vilchez
jvn00003@red.ujaen.es

Francisco J. Martínez-Moreno
fjmmoreno@ucm.es

M. Carmen Hidalgo
chidalgo@ujaen.es

[1] Department of Mechanical and Mining Engineering and CEACTEMA, Higher Polytechnic School of Linares, University of Jaen, Technological Scientific Campus, Linares, Jaen 23700, Spain

[2] Department of Geology and CEACTEMA, Higher Polytechnic School of Linares, University of Jaen, Technological Scientific Campus, Linares, Jaen 23700, Spain

[3] Department of Geodynamics, Stratigraphy and Paleontology, Faculty of Geological Sciences, Complutense University of Madrid, Ciudad Universitaria, Madrid 28040, Spain

## Introduction

Until a few decades ago, the enormous volume of waste generated in mining districts (tailings, flotation sludge, foundry slag, etc.) were allowed to accumulate near these facilities without any type of corrective measures. Furthermore, at the time of mine closure, planning measures involving the isolation of these waste accumulations were not considered. Under these conditions of exposure to the atmosphere, oxidation of the sulphides present in the waste has very negative consequences for the environment due to the generation of leachate with high contents of sulphates and certain metallic elements. These processes have been described worldwide in different abandoned mining districts (Sobanska et al. 2000; Li and Thornton 2001; Chopin and Aloway 2007).

At present, this environmental problem suggests the need to take caution measures, among which are those aimed at isolating these deposits to avoid precipitation infiltration.

Published online: 21 June 2025

Thus, it is very important to know both the geometry of the base, and the internal structure and lateral extension of these mining tailings. To characterize these mining dams, numerous studies have used indirect methods (geophysical methods) because they are useful, fast and cost-effective for reconstructing the configuration of anomaly generating bodies, identifying areas of recharge and discharge, and determining the morphology of the contacts between the residues and substrate. Among these methods, electrical tomography (ERI) is the most widely used and has been demonstrated to be effective in different mining districts (Martínez-Pagán et al. 2009; Martínez et al. 2014, 2016; Zarroca et al. 2015; Rey et al. 2020, 2022; Mendoza et al. 2023; Oliveira et al. 2023).

As mentioned, electrical tomography is a very useful technique with a vertical resolution that it is conditioned by the separation between electrodes. Thus, the smaller the electrode spacing is, the higher the resolution achieved, while the greater the separation is, the greater the depth (Sasaki 1992). In this study, a Wenner-Schlumberger electrode configuration was adopted, due to its good performance and stability against both vertical and horizontal changes in resistivities (Dahlin and Zhou 2004; Loke 2014). However, the need to use numerous electrodes, as well as to assemble and disassemble the entire device, makes field work laborious and time-consuming. In practice, this is a limitation that means that many of the studies carried out do not obtain many profiles. The number of data in the horizontal is scarce because it depends on the number of profiles performed. Therefore, the interpolation between profiles produces a low definition of correlation. For this reason, in this work we use magnetometry as a complementary method because the data acquisition is very fast, and numerous profiles can be obtained over short period. However, there are very few examples in the literature describing its use for analysing the geometry and structure of mining dumps (Yurkevich et al. 2022).

In this study, the metallogenic district of La Carolina (southern Spain, province of Jaen, Fig. 1), which is characterized by the presence of phylonian deposits consisting mainly of galena (PbS), was chosen for the geophysical characterization of the infill thickness of some taillings dams. These mineralizations have historically been the objects of intense exploitation and were abandoned at the end of the 1960s. The abundance of these sulfide deposits favoured the development of important underground mining for centuries (very important between the 19th and 20th centuries), and this activity produced a large quantity of tailings, which were deposited near the extraction sites (Gutiérrez-Guzmán 2007). The mining system used in the district was the shrinkage stoping or cut and fill stoping method. With the ore and host rock obtained from exploitation, comminution and classification operations were carried out as a step prior to the gravimetric concentration process, from which mixed and enriched waste rocks were obtained that were subsequently treated in a flotation process after milling. Through the flotation process, gangue and ore with a particle of < 1 mm and no commercial value were obtained and deposited in tailings dams. As described in previous studies (Hidalgo et al. 2006, 2010; Rojas 2019), in this mining area, there is environmental degradation related to potentially toxic elements (PTEs) that affects the quality of water and soils, similar to what has been previously found in other regions (Sobanska et al. 2000; Li and Thornton 2001; Chopin and Aloway 2007).

In this sector, a magnetic prospecting is carried out on an old tailings dam (La Manzana). This waste is composed of materials from the host rock and the mineral paragenesis that could not be separated in the flotation process. It has a very fine granulometry from the milling process.

The main goal of this study is the analysis of the effectiveness of the Earth's magnetic field to identify the thickness and depth of the mine wastes accumulated on the rock substrate and, therefore, to evaluate the interest of its application to define accurately the volume and geometry of these deposits. In order to determine the effectiveness of this method, the obtained results are compared with direct data and previous electrical prospecting data.

## Geological context and description of the tailings dam

The study area is situated on the southernmost part of the Central Iberian Zone (Julivert et al. 1972; Diez Balda et al. 1990) (Fig. 2a). The La Carolina mining district is located on the southeastern slope of Sierra Morena, on the southeastern limit of the Hesperian massif (Julivert et al. 1972; Tamain 1972) (Fig. 2b). Regionally, it is possible to differentiate the existence of two large sets of materials: a Palaeozoic basement and a post Hercynian sedimentary cover. The Palaeozoic basement consists of a succession of metasedimentary rocks (mainly phyllites and quartzite) of Ordovician to Carboniferous age (Castelló and Ortiz 1976; Fontboté 1982; Lillo 1992; Rey et al. 2005) intruded by a granite at the end of the Hercynian Orogeny (Castelló and Ortiz 1976). The post Hercinian cover, which is arranged subhorizontally and discordantly over the Palaeozoic basement, appears to have fossilized the mineralizations. It is exclusively composed of Triassic, Miocene and Quaternary materials.

The origin of the phylonian field in La Carolina is associated with extensional conditions, and the anomalous geothermal gradient originated at the end of the Hercynian Orogeny. These mineralizations are of hydrothermal origin,

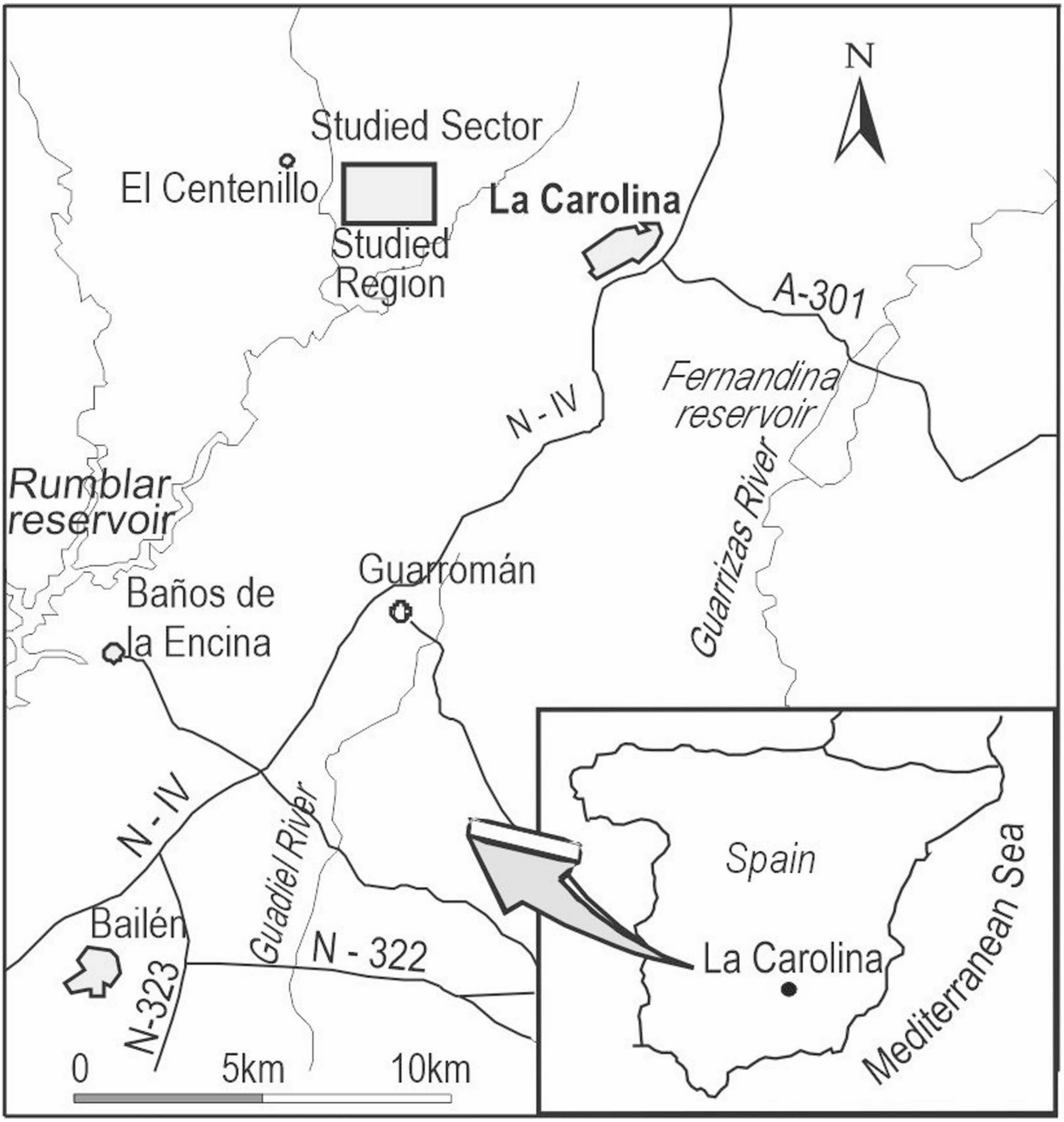


**Fig. 1** Location of the studied region

where the fluid phase and the metals were injected through fractures and discontinuities in the granite mass and the Palaeozoic host rocks. The paragenesis of the ore primarily consists of galena, with minor proportions of sphalerite, pyrrhotite, chalcopyrite and pyrite. Quartz, ankerite and calcite predominate as gangue minerals (Lillo 1992).

In this work, one of the largest waste accumulations stored in the mining district, known as La Manzana, was selected (Fig. 2c). It is a tailings dam with a size of approximately 250 × 400 × 20 m and a waste volume of approximately 2,000,000 $m^3$ (Fig. 3a), and its deposits rest directly on Silurian phyllites. This waste accumulation occupies a basin through which an old stream runs, and the runoff waters are channelled through a pipe at the bottom of the tailings dam. The top surface is flat (Fig. 3a). Mining waste consists of fine rejected material generated in the galena ore

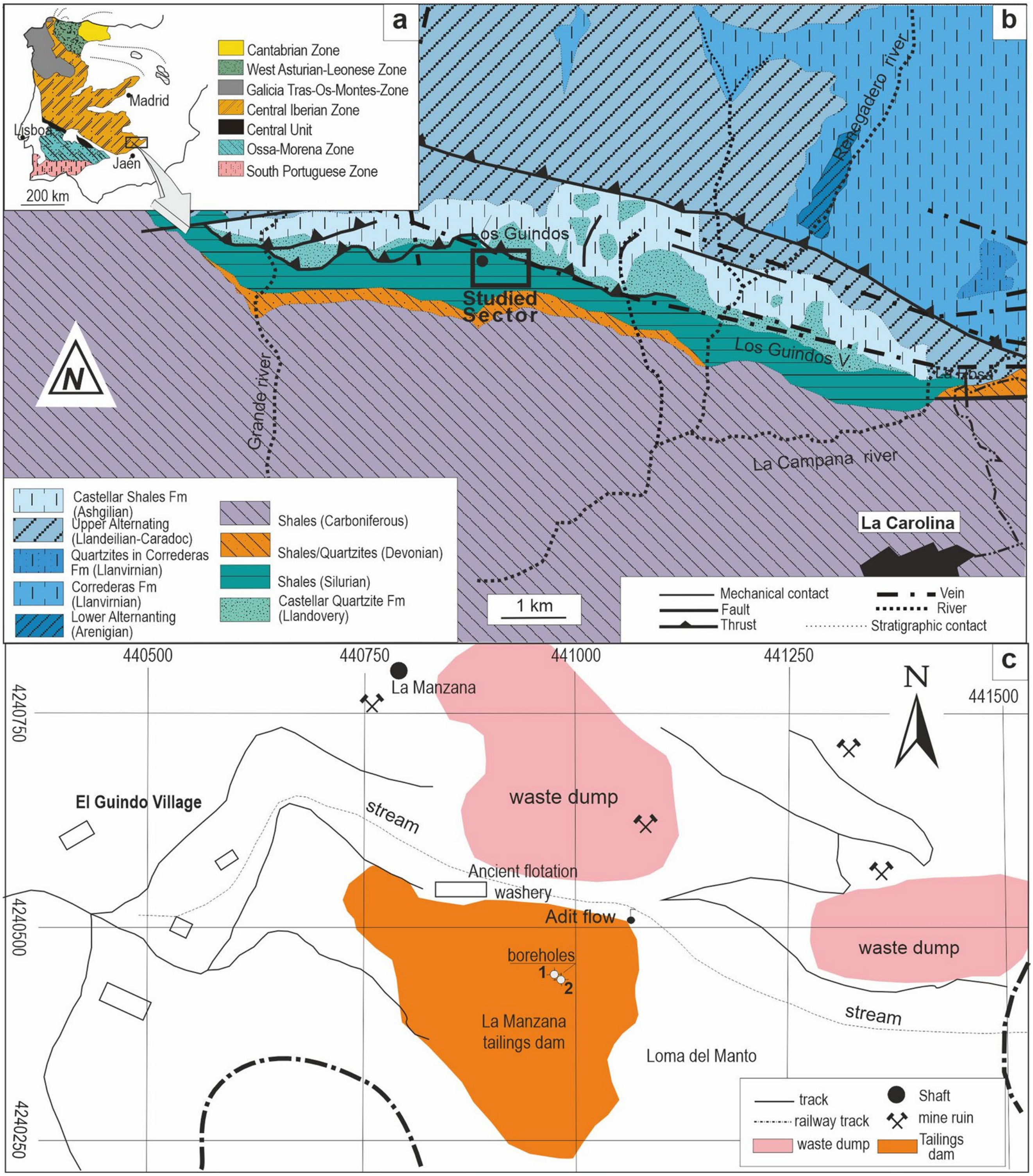


**Fig. 2** (**a**) Geological context from Diez Balda et al. 1990, (**b**) regional geological map. (modified from Castelló and Ortiz 1976) and (**c**) details of the location of the La Manzana tailings dam in the study area


**Fig. 3** Photographs. (**a**) General view of the tailings dam. (**b**) Upper part of the chimney drain installed in the tailings dam. (**c**) Details of the drainage at the foot of the tailings dam. (**d**) Field procedure used for magnetic data collection using the GSMP magnetometer

concentration process via the flotation method. Non-recoverable minerals as pyrite, chalcopyrite and pyrrhotite are included as sterile particles.

The structure was built via upstream regrowth from a small dam consisting of coarse materials. The discharge system consisted of a gutter (via gravity) in the outer portion of the structure and the drainage system consisted of a lateral chimney, which is still preserved (Fig. 3b), and PVC drain pipes connected to the bottom pipe. There is a mine drainage gallery at the foot of the dam (Fig. 3c), whose discharge is maintained throughout the year, even in the dry season. It corresponds to the saturated zone of the dump and the drainage of an old mine adit buried under mining waste (Rojas 2019). The magnetic field surveying conducted in this work were carried out on tailings that fossilized all of these structures and currently have a completely horizontal ceiling morphology (Fig. 3d).

## Previous studies and characterization of the tailings dam

The La Manzana dam has been the subject of previous studies related to analysing the contamination potential of mining wastes (Martínez et al. 2014; Rojas 2019). Geochemical characterization of the sediments indicated that this tailings dam has high concentrations of metal(loid)s, such as Fe (25000 mg/kg), Pb (8000 mg/kg), Zn (5000 mg/kg), Mn (500 mg/kg), and As (500 mg/kg). In addition, these tailings present pH values of approximately 8 due to the presence of additives, such as $CaCO_3$, that were used for the extraction of galena.

Two boreholes were drilled in the central area of the dam, at a distance of four metres from each other to reach the metamorphic substrate. The first borehole was drilled with a triple battery to obtain an unaltered continuous core that enabled the acquisition of samples for granulometric, geochemical and mineralogical analyses. It reached the

Palaeozoic substrate at 29 m of drilling. Sensors for measuring humidity, pore water electrical conductivity, temperature and dissolved oxygen were installed at different depths. This set of sensors enabled the variations in these parameters to be recorded over more than a decade, and the evolution of the geochemical processes within this tailings dam was analysed. The second borehole was used as a piezometer for measuring the water table and taking water samples in the saturated zone of the dump. The boreholes cut the phyllites at 27.50 m during drilling. This direct information is used as correlation data with indirect research techniques. The depth of this contact, together with the information provided by the old aerial photographs prior to the construction of this dam (Fig. 4a), are essential tools for the adequate interpretation of geophysical prospecting profiles (Fig. 4b and c).

The tailings are primarily constituted by gangue of the exploited mineralization (quartz, calcite, ankerite, feldspars and phyllosilicates) and those sulfide ores (pyrrhotite, pyrite and chalcopyrite) that were not of economic interest. Galena and cerussite also appears, but in low proportion, as trace minerals (Rojas 2019). Total sulfide content does not exceed 0.3% in the tailings dam, although this value is above the limit established by the European Union in its directive 2006/21EC for wastes. $CaCO_3$ values are between 3% and 6%. In the case of the texture presented by these sediments, it should be noted that it is mostly made up of sand, with a low content in silt and clay (Fig. 4d). Oxygen sensors installed in the dump at different depths indicate that the oxidation front is limited to the first 6–8 m. Thus, most of the waste is deposited under reducing conditions.

In the lower part of the piezometer, approximately 90 cm of water saturation occurs during the humid season. The analyses revealed very high contents of $SO_4^{2-}$ (>2900 mg/L), and dissolved Fe (>27 mg/L) and Mn (>4 mg/L) in this water (Rojas 2019).

In relation to the resistivity studies, Fig. 4c shows an electrical tomography profile of this tailings dam that was obtained in a previous work (Martínez et al. 2014). Two sets can be differentiated in the vertical direction: a more superficial set, with generally low-medium resistivity, which is associated with the tailings (values less than 100 Ω.m.) or a highly altered substrate (values within 80–150 Ω.m.). In the lower part, there is another set characterized by increasing resistivity values, which is related to the phyllites of the unaltered substrate (values up to 150 Ω.m.). Thus, through the ERI profile, it has been possible to detect, under the flat top of the tailings dam, the irregular morphology of the contact with the underlying bedrock at depths that vary between 10 and 40 m (Fig. 4c). The contact between the two bodies is more defined in the dry season than in the wet season, when it appears diffuse. The phyllites are very altered, so they have an important secondary porosity, and in humid periods, they can become saturated with water. This saturation favours a decrease in resistivity values and, therefore, makes them similar to those in the tailings dam (Martínez et al. 2014).

On the other hand, increases in resistivity are detected at the NW end of the dam within the tailings. These high values could be due to the presence of the peripheral dykes used for the regrowth of the waste dams (indicated as dykes in Fig. 4c). Laterally, decreases in resistivity are associated with an increase in the degree of humidity. In Fig. 4, if the position of the old ravine is compared with the position of the electrical tomography profile (Fig. 4b) and the minimum resistivity values recorded in the ERI profile (Martínez et al. 2014) (Fig. 4c), a strong correlation is observed. Thus, at approximately 220 m, the ERI profile passes through the old ravine, and it is precisely in this vertical direction where the minimum resistivity values are recorded (less than 4 Ωm).

## Magnetometry methodology

Magnetic prospecting is based on the detection of local variations (anomalies) in the Earth's magnetic field. These anomalies are caused by the petrophysical contrast, that is, the presence of materials with different magnetic susceptibility values (Telford et al. 1990; Blakely 1995). Therefore, they can be polarized by the influence of the Earth's magnetic field. As a previous step in the interpretation of the magnetometer measurements taken in the field, it is necessary to subtract the main field (the amount that is expected to exist in that place and in that moment) as well as the influence of the external fields (in this case study, only the diurnal correction). In addition, reduction to the pole was applied in order to transform the observed magnetic anomaly into an anomaly that would had been measured at the Earth's magnetic pole. This methodology has been extensively described in the literature (Telford et al. 1990; Blakely 1995; Reynolds 2011).

Magnetic prospecting is a widely used tool in different Earth science fields. In this sense, it is worth highlighting its great utility in mining and, specifically, in the prospecting of ferromagnetic elements (Fries et al. 2020; Louzada et al. 2020; Aminu et al. 2024). In addition, it has been used to carry out geological mapping in heavily covered areas (Nabighian 1988; Bouzekraoui et al. 2024), hydrocarbon prospecting sites (Okiwelu et al. 2014), archaeological prospecting sites (Pueyo-Anchuela et al. 2016; Murin et al. 2022), and locations of sinkholes or shallow holes (Mochales et al. 2005; Martínez-Moreno et al. 2014; Mendoza et al. 2023) and detection of landmines (Abdelazeem

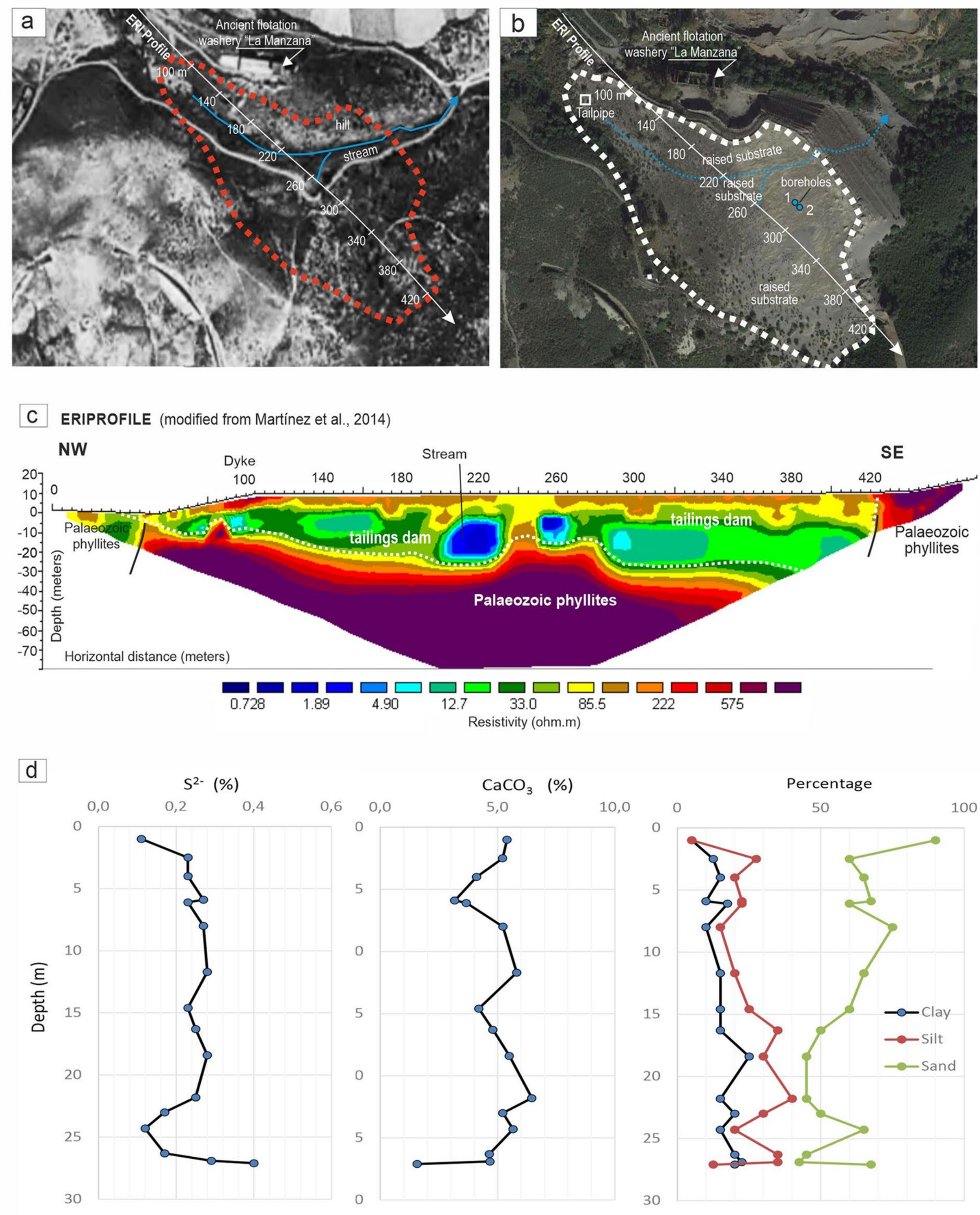


**Fig. 4** (**a**) Orthophoto from 1956–1957, obtained prior to construction of the tailings dam. The limits of the upper part of the tailings dam are indicated in red, the outline of the old ravine is indicated in blue, and the position of the electrical tomography profile is indicated in white. (**b**) Current satellite image of the tailings dam, where the positions of the old ravine, the electrical tomography profile (electrical resistivity imaging, ERI), the chimney drain, and the boreholes are indicated. (**c**) Electrical tomography profile modified from Martínez et al. 2014. (**d**) Variation with depth of selected physical–chemical parameters ($S^{2-}$: total sulfide content). Data from borehole 1

and Gobashy 2016). However, to date, it has scarcely been used to characterize mining dams (Yurkevich et al. 2022).

In this study, field work was conducted with portable magnetic/gradient equipment, model GSM Potassium of the GEM System (Fig. 3d). This potassium magnetometer offers high data quality due to its high sensitivity (0.0003 nT), minimum reading error, high resolution (0.0001 nT) and high precision (+/- 0.05 nT).

The data of the main field were obtained through calculations made by geomagnetic reference field IGRF 13 (British Geological Survey; available online; https://www.geomag.bgs.ac.uk/dataservice/home.html). To calculate the external field, the observatory of San Pablo was used as a base station (Instituto Geográfico Nacional; available online: https://www.ign.es/web/ign/portal/gmt-area-geomagnetismo).

The magnetic survey was carried out on a flat and horizontal topographic surface. The measurements with the mobile magnetometer consisted of tracing a path of 21 parallel profiles in the SW–NE direction, with continuous measurements in walking mode and a separation of approximately 15 m between the profiles (the distance was constrained by the presence of vegetation that hindered data collection). To obtain field and vertical magnetic gradient values, two sensors were used simultaneously, separated by 1 m (Fig. 3d). A vertical magnetic gradiometer is better at detecting near surface magnetic sources (Telford et al. 1990). Given the stability of the equipment that was used, measurements were taken every 50 ms for each of these profiles. Georeferencing was conducted with a NovAtel GPS device mounted on top of the mobile device (Fig. 3d).

**Table 1** Values of measured susceptibility (SI)

| Substrate | Tailings ponds (surface) | Tailings ponds (borehole) |
|---|---|---|
| 0.000101 | 0.000140 | 0.000112 |
| 0.000102 | 0.000140 | 0.000240 |
| 0.000102 | 0.000141 | 0.000452 |
| 0.000103 | 0.000141 | 0.000474 |
| 0.000106 | 0.000142 | 0.00175 |
| 0.000109 | 0.000142 | 0.000135 |
| 0.000110 | 0.000143 | 0.000194 |
| 0.000111 | 0.000143 | 0.000244 |
| 0.000112 | 0.000144 | 0.000237 |
| 0.000113 | 0.000141 | 0.000144 |
| 0.000114 | 0.000160 | 0.000221 |
| 0.000116 | 0.000155 | 0.000229 |
| 0.000117 | 0.000155 | 0.000217 |
| 0.000120 | 0.000156 | 0.000274 |
| 0.000130 | 0.000157 | 0.000278 |
| 0.000134 | 0.000157 | 0.000185 |
| 0.000134 | 0.000158 | 0.000199 |
| 0.000135 | 0.000159 | 0.000243 |
| 0.000135 | 0.000159 | 0.000320 |
| 0.000136 | 0.000160 | 0.000180 |
| | 0.000157 | 0.000373 |

To obtain the total magnetic field anomaly, the main magnetic field (obtained using the IGRF-13 model) and the contribution of the external fields (information obtained at the San Pablo base station) were subtracted from the values measured with the magnetometer at each point. The total magnetic field anomalies were calculated by means of Oasis Montaj software following a standard procedure, including reduction to the pole. Surfer software was used for data interpolation. The data were analysed with the different interpolation methods that best adapt to these data (kriging, cokriging, natural neighbour, nearest neighbor, etc.). Finally, the interpolation method selected was kriging. The variogram was studied and it showed the best adjustment with respect to the maximum distance.

To study the magnetic susceptibility, magnetic susceptibility values of various types of rocks from the substrate, surficial mining residues and borehole core samples were measured. The equipment that was used was a portable hand-held susceptometer, model Terraplus KT-10.

Different software packages were used for data modelling (Grauch and Hudson 2011; Okiwelu et al. 2014; Carrasco et al. 2023). In this work, Mag2dc software (Cooper 1997; Anwar et al. 2022), which can be downloaded (https://www.researchgate.net/publication/255696606) was used.

## Results and discussion

### Magnetic susceptibility

Magnetic susceptibility was measured in the rock substrate outcrop, the surface of the tailings dam and borehole core samples (Table 1). The data obtained have been analysed by univariate statistics to determine the central tendency and dispersion of the data for each group of materials.

The substrate is made up of low-grade metamorphic rocks, with a lepidoblastic texture. The mineralogical composition is determined by the presence of phyllosilicates (mainly muscovite, chlorite, illite and sericite) with small crystals of quartz and graphite. Tourmaline, zircon, apatite or biotite may appear as accessory minerals. The presence of diamagnetic (quartz, apatite) and paramagnetic minerals (muscovite, chlorite, tourmaline and biotite) means that a low magnetic susceptibility is expected for these facies.

In total, 20 sets of magnetic susceptibility measurements on Silurian phyllites were taken in the immediate area near the waste dump. The minimum value is $0.101 \times 10^{-3}$ SI and the maximum value is $0.136 \times 10^{-3}$ SI, the range being $0.035 \times 10^{-3}$ SI. The mean is $0.117 \times 10^{-3}$ SI and the median, with a value of $0.114 \times 10^{-3}$ SI, is shifted to the left of the mean. The standard deviation presents a value of $0.0125 \times 10^{-3}$ SI.

Twenty-one sets of magnetic susceptibility measurements were also obtained from the tailings (Table 1). The measurements were always taken in the superficial part of the dump and, therefore, on the oxidized tailings. However, the results from the sensors installed in the borehole at different depths and the results of the obtained cores indicate that from approximately 8 m depth, the materials are under reducing conditions up to the base of the borehole (at this point, up to a depth of 27.5 m). Under these reducing conditions, which constitute nearly the entire tailings impoundment, higher concentrations of magnetic minerals and therefore increased susceptibility values are expected (Orgeira et al. 2003).

In the superficial part of the tailings dam, these wastes have a minimum value of $0.140 \times 10^{-3}$ SI and a maximum value of $0.160 \times 10^{-3}$ SI, with a range of $0.020 \times 10^{-3}$ SI (Table 1). The mean is $0.150 \times 10^{-3}$ SI and the median, with a value of $0.155 \times 10^{-3}$ SI, is shifted to the right of the mean. These susceptibility values are even higher when the measurements are carried out on the borehole core samples (Table 1): a minimum value of $0.112 \times 10^{-3}$ SI is registered in the reduced zone of the dump, under the oxidation front, with a maximum value of $1.75 \times 10^{-3}$ SI. The mean is $0.25 \times 10^{-3}$ SI and the median, with a value of $0.24 \times 10^{-3}$ SI, is quite close to the mean. Both values are substantially higher than that obtained for the substrate rocks.

## Magnetic prospecting

The total field magnetic anomalies are represented in Figs. 5 and 6. In Fig. 5, three of the twenty-one SW-NE profiles obtained from the tailings dam and one profile N-S are shown, and their positions are indicated in Fig. 6 (profiles 6, 8, 14 and N-S). They were selected for their proximity to the boreholes (profile 6), for coinciding with the known irregular geometry of the Palaeozoic substrate (profiles 8 and 14), and for getting a real perspective of the geometry (profile N-S). In each profile, the total field magnetic anomaly (expressed in nT) and the vertical magnetic gradient (expressed in nT/m) are represented. When the total field magnetic anomaly profiles and the vertical magnetic gradient profiles that appear in the respective figures are compared, no major differences are detected. The trends in the curves are very similar, although the magnitude of the anomaly can change.

In profile 6, very similar trends are observed when comparing the total field magnetic anomaly and vertical gradiometric values, with minimum total field magnetic anomaly values at the beginning of the profile that coincide with the periphery of the dam (SW sector), increasing the thickness and magnetic anomaly values towards the NE. At 132 m from the origin, a very significant, narrow and steep anomaly is observed, that is detected in both magnetic and gradiometric modes and coincides with the position of the boreholes 1 and 2 (related to the presence of materials with ferromagnetic behavior inside the boreholes).

In profile 8, a maximum value is observed in the total field magnetic anomaly approximately 129 m from the origin. If the position of this maximum in Fig. 5 is compared with that of the ravine (Figs. 4 and 6), they coincide. From this point forwards, the thickness of the dam decreases due to the height of the substrate, as shown in Fig. 4a. This decrease in thickness is correlated with the decrease in the anomaly in the final part of profile 8 (Fig. 5). The vertical magnetic gradient trend is inverse from the beginning to 34 m, but for the rest of the profile both trends are similar. It could be associated with the presence of very superficial buried elements, which due to their position could correspond to old drainage pipes, currently totally hidden,

In relation to profile 14 (Fig. 5), an upward and subsequent downward trend is recorded in both the magnetic anomaly and the vertical magnetic gradient. The trace of the old ravine is very well identified (Figs. 4 and 6), coinciding with a maximum value at 43 m for the magnetic anomaly, which would correspond to the maximum thickness of the residue and, therefore, to the deepest part of the old relief. In the case of vertical magnetic gradient, a very high anomaly of low amplitude is observed at 8 m from the SW: it could correspond to some superficial metallic element of anthropogenic origin unrelated to the residue.

In profile N-S (Fig. 5), the magnetic anomaly shows an increasing trend until it reaches the maximum value 30 m from the origin, which coincides with the bed of the old ravine. The minimum value of magnetic anomaly is recorded at 170 m from the origin, in the south of the profile, and corresponds to the crest of the natural slope of the rocky substrate.

Figure 6 shows two anomaly maps (the total field magnetic anomaly map in Fig. 6a and the gradiometric anomaly map in Fig. 6b) on a digital image from Google Earth. Figure 6c shows a 3D map of total field magnetic anomaly. These anomaly maps were prepared with the Surfer program using the total of the registered profiles. The figure also indicates the position of the old ravine, as well as the four profiles discussed above. A comparison of these Figs. 6a and c with those in Fig. 4a and b reveals that the lowest values of the total field magnetic anomaly coincide in the North sector with the elevation of the substrate in Fig. 4a, and therefore, with the smallest thickness of the tailings, which coincide with the southern limit of the dump, where there is another topographic high, which constrains the decrease in the thickness of the fill.

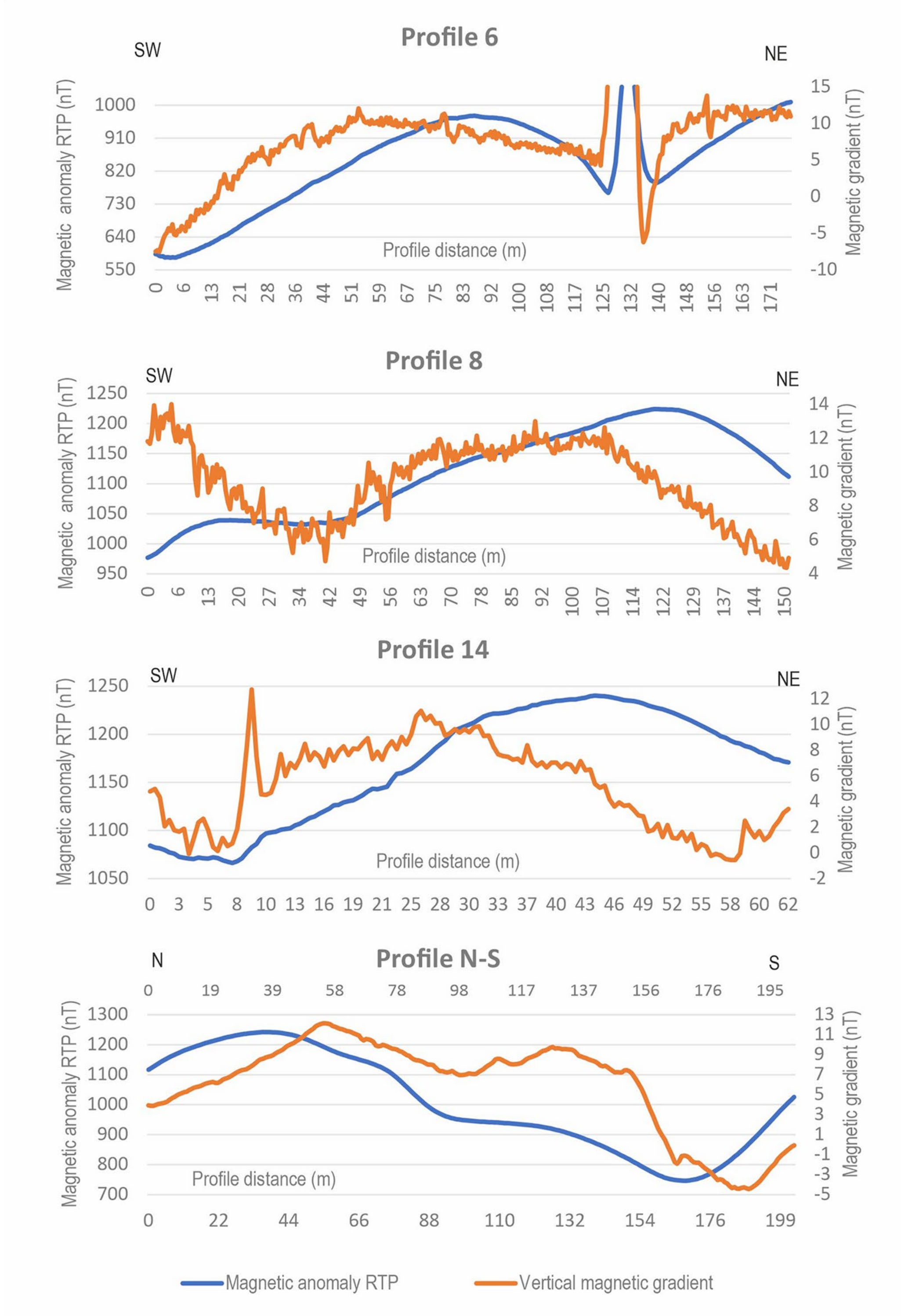


**Fig. 5** Graphs representing four of the total field magnetic anomaly curves created for the dump. Data for profiles 6, 8 and 14 were measured in the field. Profile N-S was obtained from data measured in the SW-NE profiles. The positions of each component are shown in Fig. 6. For each of these profiles, both the total field magnetic anomaly (blue line) and the magnetic gradient (brown line) are represented

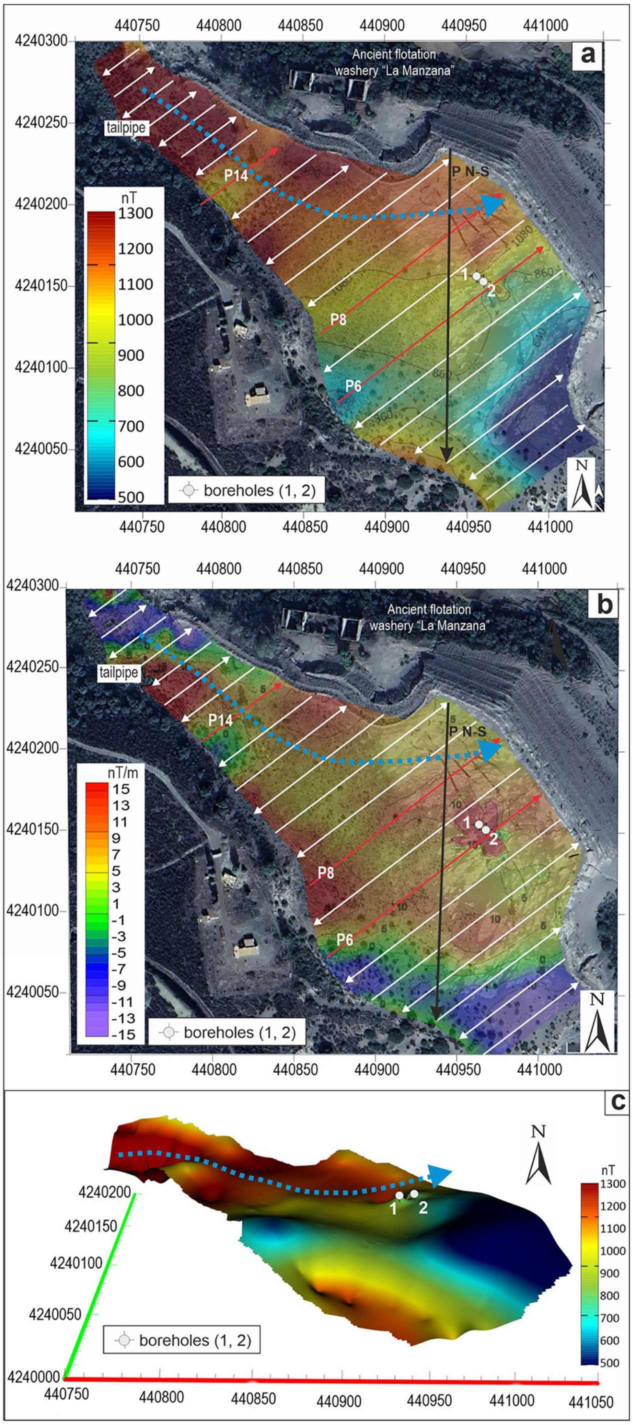


**Fig. 6** Total field magnetic anomaly map (**a**) and magnetic gradient (**b**) shown on the current satellite image of the dump. (**c**) The position of the old ravine is indicated (blue dashed line), and the 21 magnetic SW-NE profiles and profile N-S are shown. The profiles included in Fig. 5 are represented by red lines (P6, P8 and P14) and a black line (profile N-S)

Therefore, there is a correlation between the magnetic anomaly values and the thickness of the sediments in the mining dam.

## Modelling of Mag2dc profiles

Modelling of the magnetic anomaly curve of the profile N-S (Figs. 5 and 6) was carried out using Mag2dc software that allows to apply forward modelling in 2D. Two main bodies with very different magnetic susceptibilities have been considered: on the one hand, the substrate, with low values, and on the other hand, the tailings dam, with higher values. The changes in the susceptibility and morphology of both bodies will allow the field curve and the one obtained in the modelling to be adjusted. However, we do not know precisely the value of susceptibility in the unoxidized core of the dump, since the borehole samples show a certain degree of alteration and there is a wide range of measured values (Table 1). Nevertheless, we do know that this body offer values of magnetic susceptibility higher than those of the substrate and even higher than those measured in the tailings from the core samples (partially altered after ten year of exposition since the borehole drilling). In addition, it should be considered in the model that there are other structures associated with the old drainage of the dump, built with bricks and metal elements, and therefore, with very high values of magnetic susceptibility. Some of these elements are visible on the surface (Fig. 3b). Others may be shallow, both affecting the magnetic field.

To perform the modeling, it is also necessary to know the changes in the thickness of the tailings. To this end, in addition to the data from the electrical tomography and the information from the field surveys, the orthophoto of Fig. 4a, taken prior to the construction of the mining dump, is also used. This photo helps to deduce the geometry of the base of the dump: the position of the old ravine (now channeled and buried under the tailings), an elevated area in the northern sector (where the ruins of the old washery currently appear), as well as the elevated areas of the southern sector, can be detected.

The model presented in Fig. 7 was carried out using the values of the magnetic anomalies (reduced to the pole) in the profile N-S (see Figs. 5 and 6). For the layout of the profile, it is considered that the maximum thickness of the material accumulated in the dump would coincide with the position of the ravine. From this point towards the peripheral areas (both to the north and to the south) the thickness diminishes. The profile also shows two small bodies of high susceptibility (3 and 4 in Fig. 7) associated with the old drainages. In this sense, in the N-S magnetic gradient profile (Fig. 5) two maxima are detected (about 60 and 130 m from the origin) that could be associated with these structures.

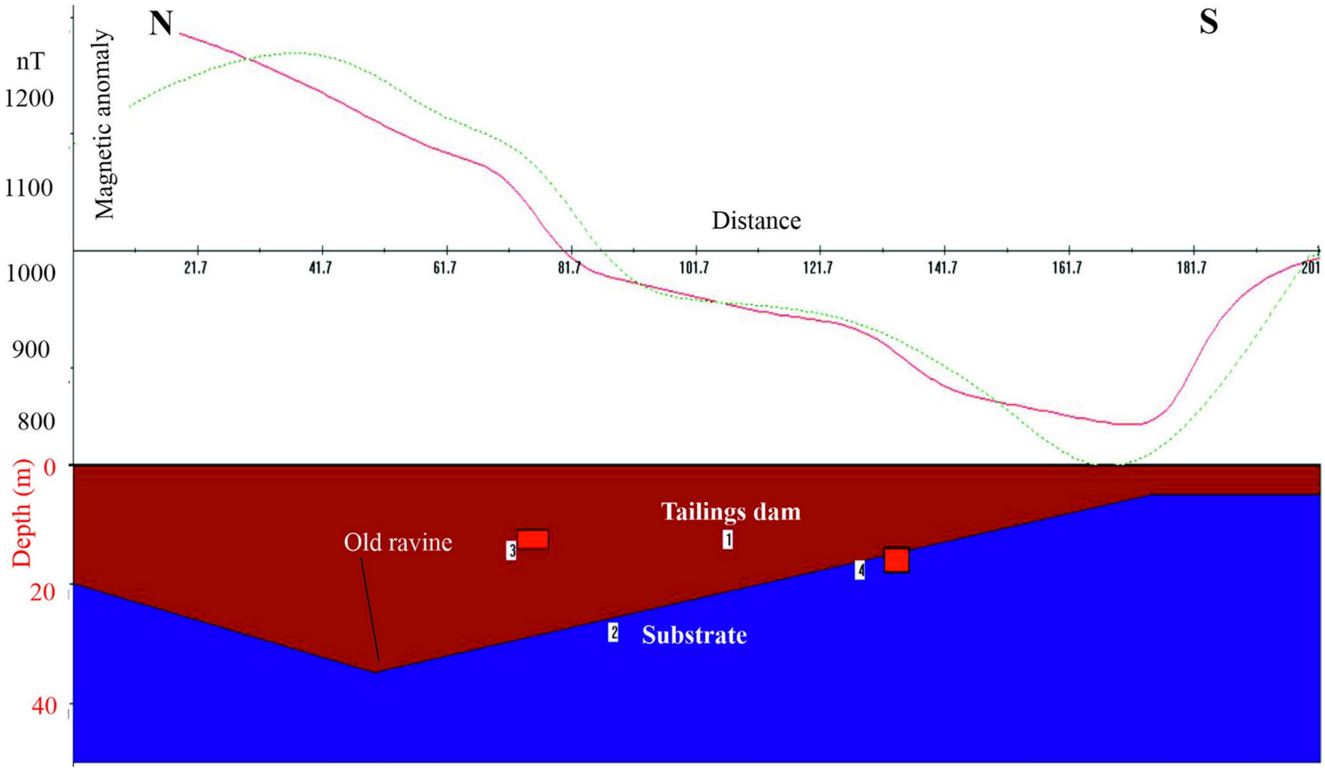


**Fig. 7** Comparison of the total field magnetic anomaly curve in profile N-S reduced to the pole (green dashed line) and the curve obtained by the Mag2dc software for the considered substrate model (red line). The position of the ravine is indicated. 1: Substrate. 2: Tailings dam. 3 and 4: Drainage pipes. Magnetic susceptibility: 3–4 > 1 > 2

In Fig. 7, the values for this profile are represented by a green dashed line, and the resulting magnetic anomaly curve from the modelling is represented by a solid red line. It should be noted that, except for the extremes, both curves have a good fit. This finding confirms that negative magnetic anomalies are associated with the height of the substrate, thus allowing variations in the morphology of the base of the mining dump to be identified. In this profile, a topographic difference of approximately 30 m is estimated (Fig. 7).

## Conclusions

In this work, different geophysical methods (previously published electrical and new magnetic data), old orthophotos, direct information from mechanical boreholes and direct data taken from outcrops are integrated and compared to analyse the applicability of magnetometry in the modelling of geological structures with mining potential. Specifically, the ability of these methods to deduce the base geometry on which an old flotation sludge dam was deposited is studied. For this purpose, the old mining district of La Carolina (southeastern Spain), where the Philonian deposits of galena were exploited, was chosen.

In this study a correlation between total field magnetic anomaly values and changes in the accumulated thickness of mining waste was established. In this example, the lowest magnetic values coincide with the smallest thicknesses of the tailings dam. As the roofs of these tailings dams are flat surfaces, the changes in thickness are directly related to irregularities in the roof of the rocky substrate.

This result was verified by comparing the magnetic anomaly curves obtained in the field with the theoretical curves obtained with the proposed geometric model, which were calculated using the Mag2dc program. This comparative study shows the usefulness of magnetic prospecting in characterizing the base geometry of these mining structures and, therefore, its application to environmental characterization studies.

**Author contributions** Conceptualization, R.M. and J.R.; methodology, R.M, J.R. and M.C.H.; statistical analysis and software, R.M. and F.J.M.; investigation, R.M., J.V., J.R. and M.C.H.; writing original draft, J. Rey and M.C.H.; writing - review & editing, R.M., M.C.H. and J. Rey. All authors have read and agreed to the published version of the manuscript.

**Funding** Funding for open access publishing: Universidad de Jaén/CBUA. Funding for open access publishing: Universidad de Jaén/CBUA. Grant PID2021-123506OB-I00 was funded by the MICIU/AEI/https://doi.org/10.13039/501100011033 and ERDF/EU. The study was partly funded by the University of Jaen.

**Data availability** The data that support the findings of this study are available upon request from the corresponding author, J.R.

## Declarations

**Conflict of interest** The authors declare that they have no conflicts of interest that could have inappropriately influenced this work.



## References

Abdelazeem M, Gobashy MM (2016) A solution to unexploded ordnance detection problem from its magnetic anomaly using Kaczmarz regularization. Interpretation 4(3):61–69. https://doi.org/10.1190/INT-2016-0001.1

Aminu MB, Adiat KAN, Akinlalu AA, Olomo KO, Owolabi TO, Aliyu EO (2024) A review on the applications of airborne geophysical and remote sensing datasets in epithermal gold mineralisation mapping. Geosyst Geoenvironment 3. https://doi.org/10.1016/j.geogeo.2024.100284

Anwar H, Ipmawan VL, Sriyakul T (2022) Geophysical analysis using proton precession magnetometer GSM-19T as information on fault presence in medana, North lombok, Indonesia. Int J Hydrol Environ Sustain 1:08–23. https://doi.org/10.58524/ijhes.v1i1.57

Blakely R (1995) Potencial theory in gravity and magnetic applications. Cambridge University Press, p 441

Bouzekraoui M, Es-Sabbar B, Karaoui B, Essalhi M, Saadi M (2024) Structural analysis, tectonic fracturing modeling, and kinematic evolution along the South atlas fault at the Northern border of the Tinghir-Errachidia-Boudenib basin (Pre-African trough, Morocco). J Afr Earth Sc 212. https://doi.org/10.1016/j.jafrearsci.2024.105193

Carrasco J, Carrasco P, Porras D, Martín I (2023) Drone magnetic and time domain electromagnetic exploration in metamorphic formations: tool for the identification of strategic sites for aquifer exploitation. Appl Sci 13:10949. https://doi.org/10.3390/app131910949

Carvalhêdo LdaC, Chatack Carmelo L, Francisquini A, Botelho N (2020) Geophysical-geological model of the Pedra Branca Massif in the Goiás Tin province, Brazil. J S Am Earth Sci 101. https://doi.org/10.1016/j.jsames.2020.102593

Castelló R, Orviz F (1976) Mapa y memoria explicativa de La Hoja Nº 884 (La Carolina) Del Mapa Geológico de españa, Escala 1:50.000. Instituto Geológico y Minero de España.

Chopin EIB, Aloway BJ (2007) Trace element partitioning and soil particle characterization around mining and smelting areas at tharsis, Ríotinto and huelva, SW Spain. Sci Total Environ 373:488–500

Cooper GRJ (1997) Forward modelling of magnetic data. Computers Geoscience 23:1125–1129

Dahlin T, Zhou B (2004) A numerical comparison of 2D resistivity imaging with 10 electrode arrays. Geophys Prospect 52:379–398

Diez Balda MA, Vegas R, Lodeiro F (1990) Structure, autochthonous sequences, part IV Central-Iberian zone. In: Dallmeyer RD, Martínez García E (eds) Pre-Mesozoic geology of Iberia. Springer-, Berlin Heidelberg New York, pp 172–188

Fontboté JM (1982) Mapa geológico y memoria explicativa de la hoja 70 (Linares), escala 1:200.000. Instituto Geológico y Minero de España 1982

Fries M, Machado Zago M, Garcia da Silva FA (2020) Geophysical study contributing to analysis and characterization of a localized copper occurrence. J Appl Geophys 179. https://doi.org/10.1016/j.jappgeo.2020.104129

Grauch VJS, Hudson MR (2011) Aeromagnetic anomalies over faulted strata. Lead Edge 30:1242–1252. https://doi.org/10.1190/1.3663396

Gutierrez-Guzmán F (2007) Minería En Sierra Morena. Ilustre Colegio de Ingenieros Técnicos de Minas de Linares, Granada, Jaén y Málaga

Hidalgo MC, Benavente J, El Mabrouki K, Rey J (2006) Estudio hidroquímico comparativo En Dos sectores Con Minas Abandonadas de sulfuros metálicos: Distrito de Linares-La Carolina (Jaén). Geogaceta 39:123–126

Hidalgo C, Rey J, Benavente J, Martínez J (2010) Hydrogeochemistry of abandoned Pb sulphide mines: the mining district of La Carolina (southern Spain). Environ Earth Sci 61:37–46

Julivert M, Fontboté JM, Ribeiro A, Conde LE (1972) Mapa tectónico de La Península ibérica y baleares, E. 1:1.000.000, memoria explicativa. IGME

Li X, Thornton I (2001) Chemical partitioning of trace and mayor elements in soils contaminated by mining and smelting activities. Appl Geochem 16:1693–1706

Lillo J (1992) Geology and Geochemistry of Linares-La Carolina Pb-Ore field (Southeastern border of the Hesperian Massif). Ph. D. Thesis, Univ. Leeds

Loke MH (2014) Tutorial: 2-D and 3-D electrical imaging surveys, Revision date: 5th November 2014. www.geotomosoft.com

Martínez J, Rey J, Hidalgo MC, Garrido J, Rojas D (2014) Influence of measurement conditions on resolution of electrical resistivity imaging: the example of abandoned mining dams in the La Carolina district (Southern Spain). Int J Miner Process 133:67–72. https://doi.org/10.1016/j.minpro.2014.09.008

Martínez J, Hidalgo MC, Rey J, Garrido J, Kohfahl C, Benavente J, Rojas D (2016) Multidisciplinary characterization of a tailings pond in the Linares-La Carolina mining district, Spain. J Geochem Explor 162:62–71

Martínez-Moreno FJ, Galindo-Zaldívar J, Pedrera A, Teixido T, Ruano P, Peña JA, González-Castillo L, Ruiz-Constán A, López-Chicano M, Martín-Rosales W (2014) Integrated geophysical methods for studying the karst system of Gruta de Las Maravillas (Aracena, Southwest Spain). J Appl Geophys 107:149–162. https://doi.org/10.1016/j.jappgeo.2014.05.021

Martínez-Pagán P, Faz Cano A, Aracil E, Arocena JM (2009) Electrical resistivity imaging revealed the Spatial properties of mine tailing ponds in the Sierra minera of Southeast Spain. J Environ Eng Geophys 14:63–76

Mendoza R, Marinho B, Rey J (2023) GPR and magnetic techniques to locate ancient mining galleries (Linares, South-East Spain). Int J Geophys ID 6633599. https://doi.org/10.1155/2023/6633599

Mochales T, Pueyo EL, Casas AM, Soriano MA (2005) Magnetic prospection as an efficient tool for doline detection. A case study in the central Ebro basin (Northern Spain). Geological Society of London. Special Publications 279:73–84. https://doi.org/10.1016/j.jappgeo.2017.02.001

Murin I, Neumann M, Brady C, Bátora J, Čapo M, Drozda D (2022) Application of magnetometry, Georadar (GPR) and geoelectrical methods in archaeo-geophysical investigation of a Napoleonic battlefield with fortification at Pressburg (Bratislava, Slovakia). J Appl Geophys 196. https://doi.org/10.1016/j.jappgeo.2021.104493

Nabighian NM (1988) Electromagnetic method in applied geophysics. Tulsa, Okla. Soc Explor Geophys, 971 p

Okiwelu AA, Obianwu VI, Eze Ohara E, Ude IA (2014) Magnetic anomaly patterns, fault-block tectonism and hydrocarbon related structural features in the Niger Delta basin. IOSR J Appl Geol Geophys (IOSR-JAGG) 2:31–46

Oliveira LA, Braga MA, Prosdocimi G, Cunha AS, Santana L, da Gama F (2023) Improving tailings dam risk management by 3D characterization from resistivity tomography technique: case study in Sao Paulo– Brazil. J Appl Geophys 210. https://doi.org/10.1016/j.jappgeo.2023.104924

Orgeira MJ, Walther AM, Tófalo OR, Vásquez CA, Berquó TS, Favier Dobois C, Bohnel H (2003) Environmental magnetism in fluvial and loessic holocene sediments and paleosols from the Chaco-pampean plain (Argentina). J S Am Earth Sci 16:259–274

Pueyo-Anchuela O, Diarte-Blasco P, García-Benito C, Casas-Sainz AM, Pocoví JA (2016) Geophysical and archaeological charaterization of a modest Roman villa: methodological considerations about progressive feedback analyses in sites with low geophysical contrast. Archaeol Prospection 23:105–123

Rey J, Hidalgo MC, Martínez-López J (2005) Upper Ordovician-Lower silurian Transgressive-Regressive cycles of the central Iberian zone (NE jaén, Spain). Geol J 40:1–19

Rey J, Martínez J, Hidalgo MC, Mendoza R, Sandoval S (2020) Assessment of tailings ponds by a combination of electrical (ERT and IP) and hydrochemical techniques (Linares, Southern Spain). https://doi.org/10.1007/s10230-020-00709-3. Mine Water and the Environment

Rey J, Mendoza M, Martínez J, Hidalgo MC, Florez-Rodríguez C (2022) Combining geophysical methods (DC, IP, TDEM and GPR) to characterize mining waste in the Linares-La Carolina district (southern Spain). J Environ Manage 322. https://doi.org/10.1016/j.jenvman.2022.116166

Reynolds JM (2011) An introduction to applied and environmental geophysics. John Wiley and Sons Ltd., p 796

Rojas D (2019) Influence of Mine Wastes on the Water Resources in the La Carolina Mining District (Jaen). Ph. D. Thesis University of Jaen, Jaén, Spain

Sasaki Y (1992) Resolution of resistivity tomography inferred from numerical simulation. Geophys Prospect 40:453–464

Sobanska S, Ledésert B, Deneele D (2000) Laboudigue, A. Alteration in soils of slag particles resulting from lead smelting. Comptes Rendus Acad Sci Paris Série 2 Terre Planètes Fase A 33:271–278

Tamain G (1972) Recherches géologiques et minières en Sierra Morena orientale (Espagne). Thesis Univ. Paris-Sud (Orsay). Trav. Lab. Géol. Struct. Appli. 91- Orsay, 648 pp

Telford WM, Geldart LP, Sheriff RE (1990) Applied geophysics. Cambridge University Press, p 770

Yurkevich N, Osipova P, Tsibizov L, Tsibizova E, Fadeeva I, Volynkin S, Tulisova K, Kuleshova T (2022) Current state of the gold mining waste from the ores of the ursk deposit (Western siberia, Russia). Appl Sci 12(20). https://doi.org/10.3390/app122010610

Zarroca M, Linares R, Velásquez-López PC, Roqué C, Rodríguez R (2015) Application of electrical resistivity imaging (ERI) to a tailings dam project for artisanal and small-scale gold mining in Zaruma-Portovelo, Ecuador. J Appl Geophys 113:103–113